

INTERPRETING STRUCTURES OBSERVED IN PELLET ABLATION PROFILES IN THE STELLARATOR TJ-II

¹K. J. MCCARTHY, ¹I. GARCÍA-CORTÉS, ¹B. van MILLIGEN, ¹A. BACIERO, ¹R. CARRASCO, ¹T. ESTRADA, ¹R. GARCÍA, ¹J. HERNÁNDEZ SÁNCHEZ, ¹B. LÓPEZ MIRANDA, ¹F. MEDINA, ¹D. MEDINA-ROQUE, ¹M. NAVARRO, ¹N. PANADERO, ¹I. PASTOR, ¹M. C. RODRÍGUEZ, AND ¹TJ-II TEAM

¹Laboratorio Nacional de Fusión, Ciemat. Madrid, Kingdom of Spain

Email: kieran.mccarthy@ciemat.es

1. INTRODUCTION

Cryogenic pellet injection is used in magnetic confinement fusion devices to fuel the plasma core [1]. In the case of stellarators, recent evidence from TJ-II suggests a relationship between the radial location of low-order rational surfaces and post-injection enhanced performance [2, 3]. The current understanding highlights the importance of low-order surface placement with regard to the edge gradient region, as this can result in enhanced local turbulence levels that facilitate the formation of zonal flows and concomitant transport barriers. Surface localization is also of general interest, for instance, magnetohydrodynamic (MHD) modes, which are generally bad for confinement, can develop in their vicinity. Indeed, magnetic islands, which can modify electron temperature and density profiles, can also form in their vicinity. Recently, ablation profiles exhibiting significant localized dips in signal levels have been seen when a pellet is injected into TJ-II plasmas created using a magnetic configuration with major low-order rational surfaces in its core region. However, such dips disappear when a net plasma current (± 1 kA), which modifies the rotational transform profile, is present. Here, we evaluate if structures seen in pellet ablation profiles in TJ-II are associated with low-order rational surfaces, and if so, can they aid in their localization.

2. PELLET ABLATION

In the TJ-II pellet ablation is determined primarily by T_e [4]. In the case of H pellets, the ablation rate [H/s] is well described by $3.47 \times 10^{14} \cdot n_e^{0.45} \cdot T_e^{1.72} \cdot r_p^{1.44}$, where n_e and T_e are electron density [cm^{-3}] and temperature [eV], respectively, and r_p is pellet radius [cm]. During ablation, plasma particles, in particular electrons, create a cloud of H atoms that subsequently surrounds and impedes direct energy flow to the solid, thus heat transfer dominates. Plasmoids (partially ionized clouds) expand along magnetic fields before detaching and undergoing grad-B drift, this process continuing until no ice remains. Experimentally, ablation is tracked using Balmer $H\alpha$ (656.3 nm) light emitted by cloud H atoms. Such emissions provide a rough rather than an absolute estimate of ablation [5]. Nonetheless, current pellet ablation codes [6, 7], some based on the Neutral Gas Shielding model, show reasonable agreement with $H\alpha$ profiles. In addition to high-frequency signal variations, *i.e.*, striations, large dips may occur occasionally, these being associated with islands or very low-order rational surfaces. In TJ-II, large reproducible dips in $H\alpha$ profiles are seen for injections into magnetic configurations with low-order rational surfaces in its core.

3. EXPERIMENTS IN TJ-II

In experiments in TJ-II, a large reproducible dip in $H\alpha$ is observed during intact pellet injections into plasmas created using a magnetic configuration, 100_48_65, that has several low-order rational surfaces in its core. See Figure 1. For this, balanced NBI heating is used (NBI#1 and NBI#2) and plasma current, I_p , is $\leq \pm 0.1$ kA. In Figure 1, $H\alpha$

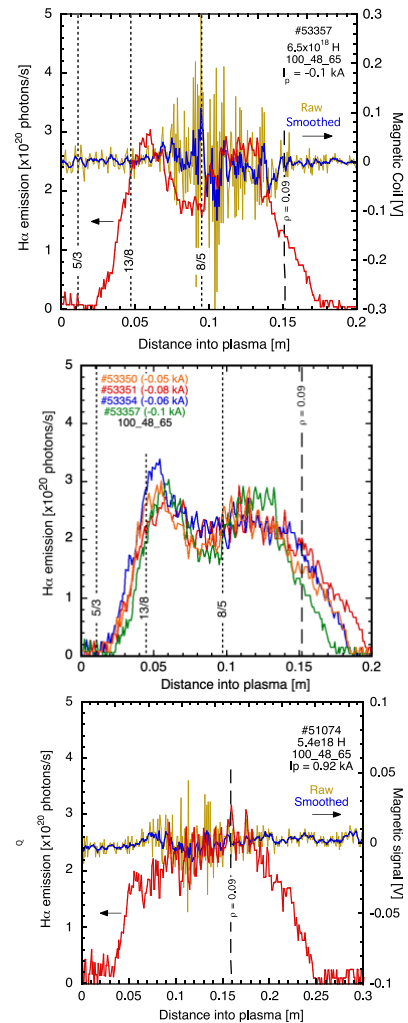


Figure 1: $H\alpha$ light and Magnetic Coil signals for pellet injections into TJ-II plasmas made with the 100_48_65 configuration. Discharges are #53357 (top), #53350, #53351, #53354 and #53357 (middle), and #51075 (bottom). Raw and smoothed magnetic signals as well as radial locations of low order rational surfaces are shown.

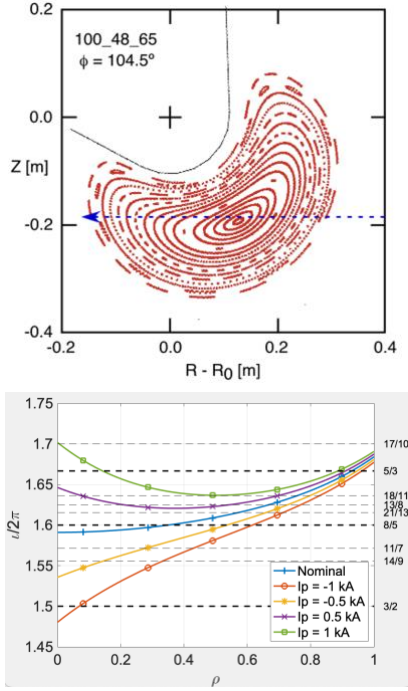


Figure 2: *Top*: Poincaré plot of magnetic field lines for the 100_48_65 configuration at the pellet injection sector of TJ-II. The nominal pellet flight path is highlighted. *Bottom*: Rotation transform profiles for 100_48_65 for vacuum and non-zero values of plasma current, I_p , (from model in Ref. [9]).

signals rise above background once a pellet has penetrated a few centimetres inside the last-closed flux-surface (LCFS), see Figure 2, this delay being attributed to low edge T_e . As the pellet penetrates deeper into hotter plasma, the $H\alpha$ signal rises steeply until a significant transient drop occurs when the ice is between 6 cm and 9 cm into the plasma. Then, once the remaining ice has traversed these radii, the signal rises again and remains at maximum until it crosses the magnetic axis. Thereafter, $H\alpha$ reduces steadily until ablation is complete. The reproducibility of this dip in $H\alpha$ points to a plasma effect rather than a pellet one (pellets exit the guide tube with a scattering cone opening angle of $\sim 0.5^\circ$ and pellet mass varies by $\leq 10\%$). In addition to this dip, other structures can be seen. For instance, fluctuations, which occur every 150 to 200 μ s and are not reproducible shot-to-shot, may be attributed to the periodic detachment of partially ionized clouds from about the ice, *i.e.*, striations [8]. Next, when distance into plasma is transposed to normalized plasma radius, $\rho = r/a$, the large $H\alpha$ drop is found to occur between $\rho = 0.67$ and 0.35 . From Figure 2, the 13/8 and 8/5 rational surfaces are present between these radii when $I_p \sim 0$ kA. In Figure 1, injections were repeated into plasmas with $I_p \sim 0.9$ kA (co-counter NBI heating only). In this case, no large dip in $H\alpha$ is seen, rather once a pellet penetrates to the hot plasma, the signal is dominated by intense fluctuations of ~ 150 kHz. In this case, I_p modifies the vacuum rotation transform profile so the 13/8 and 8/5 surfaces no longer occur within the LCFS [9 ,10]. See Figure 2.

In order to understand the physics behind these observations, comparisons with other TJ-II diagnostic techniques were carried out. It is first noted that Thomson Scattering profiles for all discharges considered here do not display significant reductions

or large-scale structures in T_e , nor in n_e , between $\rho = 0.3$ and 0.6 . Also, fast electron effects are discounted as, in TJ-II, they result in locally enhanced ablation [11]. Fast ion effects can be neglected also as $H\alpha$ dips were not observed during injections performed with the same plasma conditions for the 100_44_64 configuration ($1.56 \leq \iota/2\pi \leq 1.65$). In contrast, the presence of rational surfaces may provide a possible explanation. However, it is considered that $H\alpha$ structures associated with a pellet passing through an X-point or a rotating island should differ significantly from shot to shot and thus should not be reproducible [5]. From TJ-II data, Fast-Fourier analysis of Mirnov coil signals reveal the existence of NBI driven Alfvén eigenmodes at 133 kHz and 198 kHz just prior to pellets in discharges #53350 to #53357 and the absence of such modes in #51074 and #51075. When toroidal array magnetic coil signals are compared for these discharges, see Figure 1, large magnetic instabilities, associated with outward drifting plasmoid particles interacting with low-order rational surfaces [12], are observed for discharges #53350 to #53357 during ablation whilst such interactions are significantly reduced for discharge #51075. This points to the absence of the 13/8 and 8/5 surfaces in discharge #51074. In summary, there is first evidence that rational surfaces can be localized from pellet ablation profiles in the TJ-II.

REFERENCES

- [1] S. K. Combs and L. R. Baylor, Fusion Sci. Tech. 73, 493 (2018).
- [2] I. García-Cortés *et al.*, Phys. Plasmas 30, 072506 (2023).
- [3] K. J. McCarthy *et al.*, Nucl. Fusion 64, 066019 (2024).
- [4] K. J. McCarthy *et al.*, EPL 120, 25001 (2017).
- [5] B. Pégourie *et al.*, Nucl. Fusion 64, 056026 (2024).
- [6] B. Pégourie *et al.*, Plasma Phys. Control. Fusion 47, 17 (2005).
- [7] N. Panadero *et al.*, 58, 026025 (2018).
- [8] B. Pégourie *et al.*, Plasma Phys. Control. Fusion 49, R87 (2007).
- [9] B. van Milligen *et al.*, sent to J. Plasma Phys. for publication.
- [10] I. García-Cortés *et al.*, at this conference.
- [11] K. J. McCarthy *et al.*, Plasma Phys. Control. Fusion 61, 014013 (2019).
- [12] K. J. McCarthy *et al.*, Nucl. Fusion 61, 076014 (2021).